UNIVERSIDADE D COIMBRA

FACULDADE DE CIÊNCIAS E TECNOLOGIA

NUMERICAL ANALYSIS OF RESIDUAL STRESSES IN PARTS PRODUCED BY SELECTIVE LASER MELTING PROCESS

B.M. Marques[1] • C.M. Andrade[1] • D.M. Neto[1] • M.C. Oliveira[1] • J.L. Alves[2] • L.F. Menezes[1]

[1] University of Coimbra, CEMMPRE, Department of Mechanical Engineering, Portugal

[2] University of Minho, CMEMS, Department of Mechanical Engineering, Portugal

ESAFORM 2020
1st virtual ESAFORM 2020 conference

4th-6th May 2020
Cottbus, Germany

Additive Manufacturing

- Main **advantages** of the additive manufacturing processes:
  - ✓ Complex part geometry
  - ✓ Variety of products and materials
  - ✓ No time gap between design and prototyping

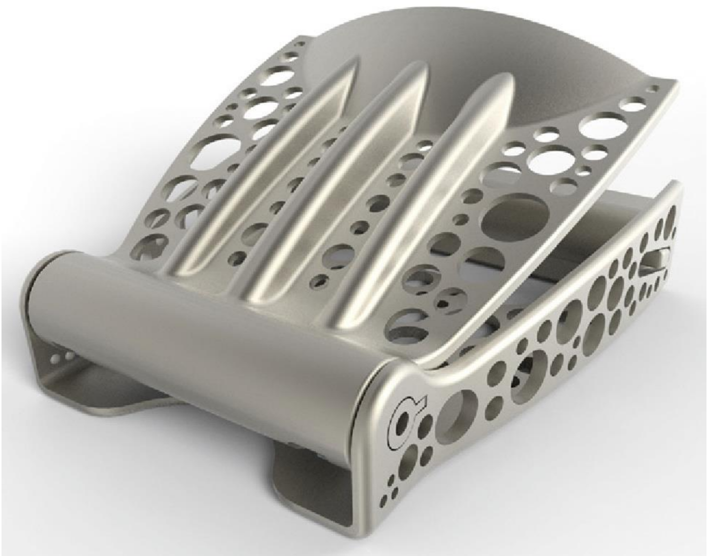

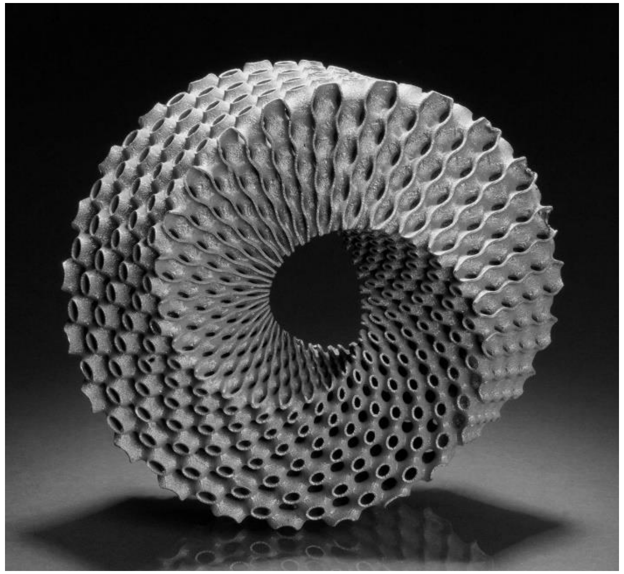

Powder-based Additive Manufacturing

- **Direct Energy Deposition**: coaxial nozzle to deliver powder to the focal point of a laser
- **Selective Laser Melting**: uses a roller to spread a thin layer of powder before melting the layer

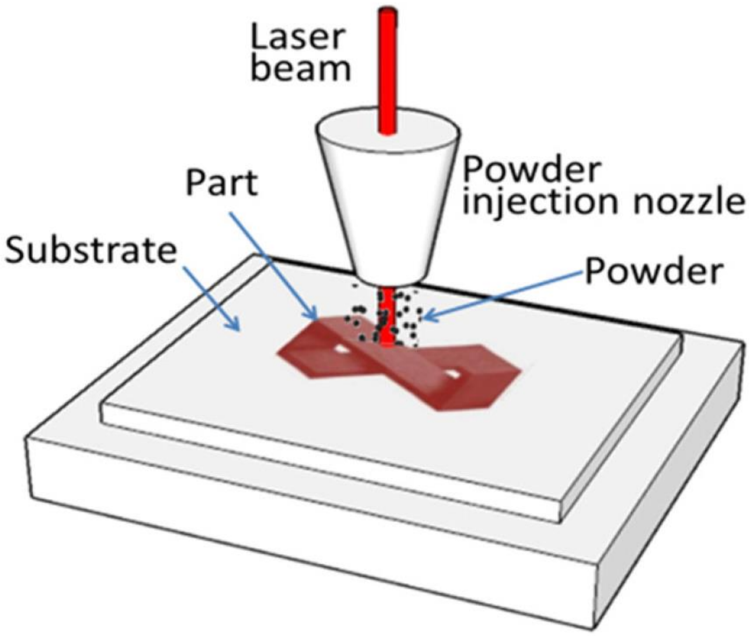

Direct Energy Deposition (DED)

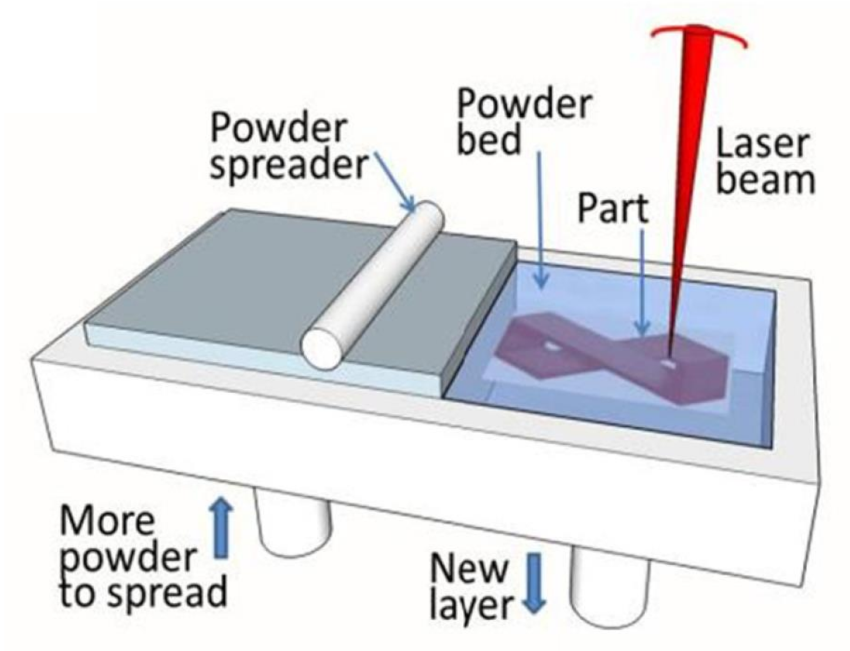

Selective Laser Melting (SLM)

Selective Laser Melting

- Example of **SLM machine** running

Selective Laser Melting

- Material phase transformation **from powder to liquid**, which then **cools down to solidification**

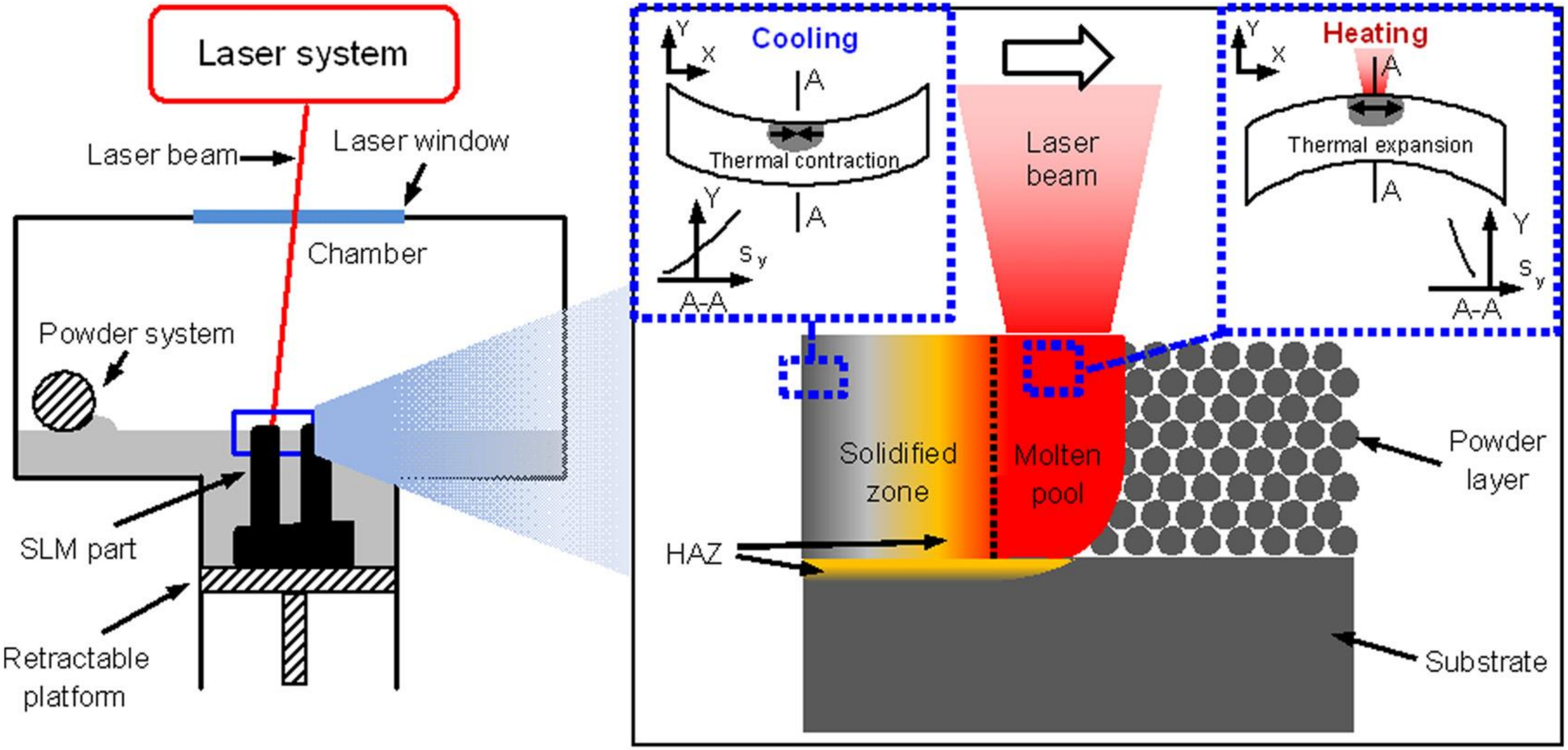

Selective Laser Melting

- The main drawback is the **high level of residual thermal stresses and large deformation** generated by temperature gradients in a layer-by-layer melting process

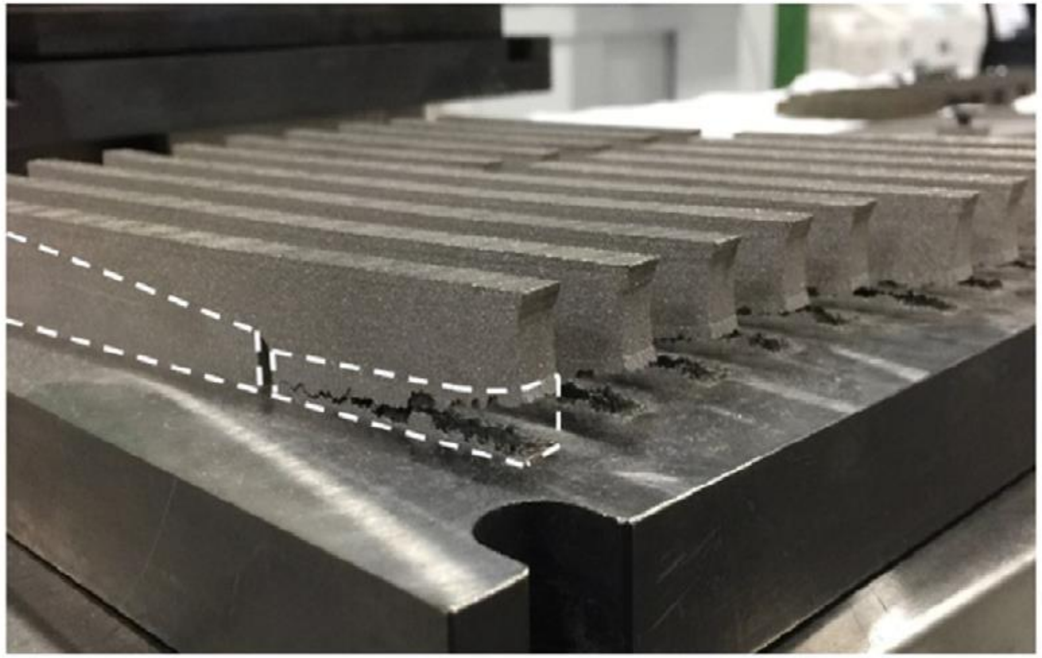

Cracks due to residual stress during the manufacturing

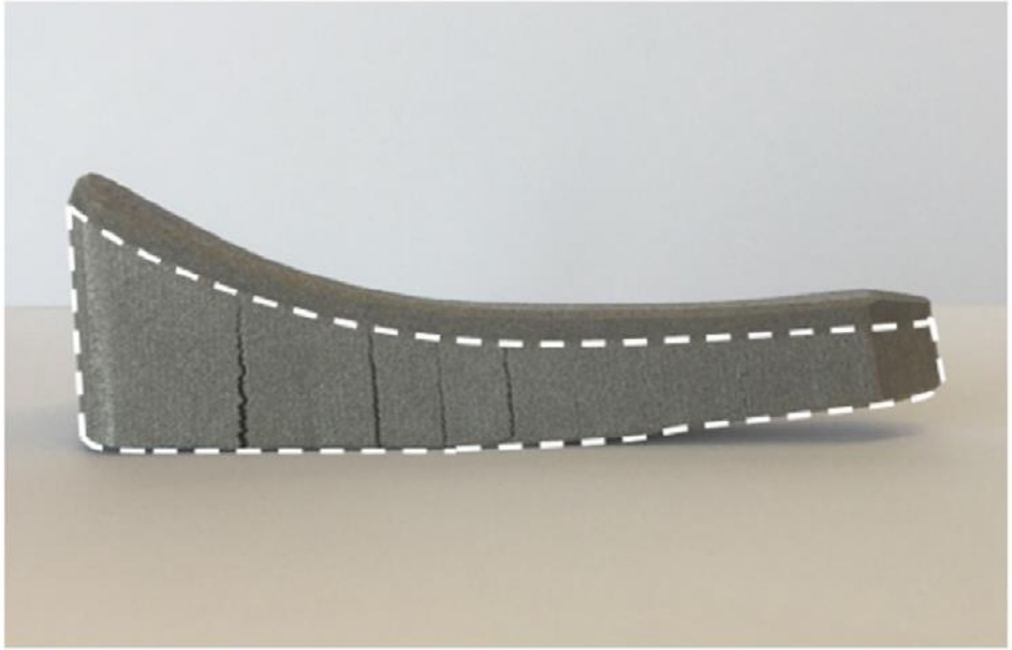

Component deformed after removal from the building chamber

SLM modelling at different length- and time-scales

- **Micro-scale:** modelling the interactions between the laser and particles
- **Meso-scale:** modelling sub-regions of the process, typically a number of scan vectors
- **Macro-scale:** modelling information for large regions or parts

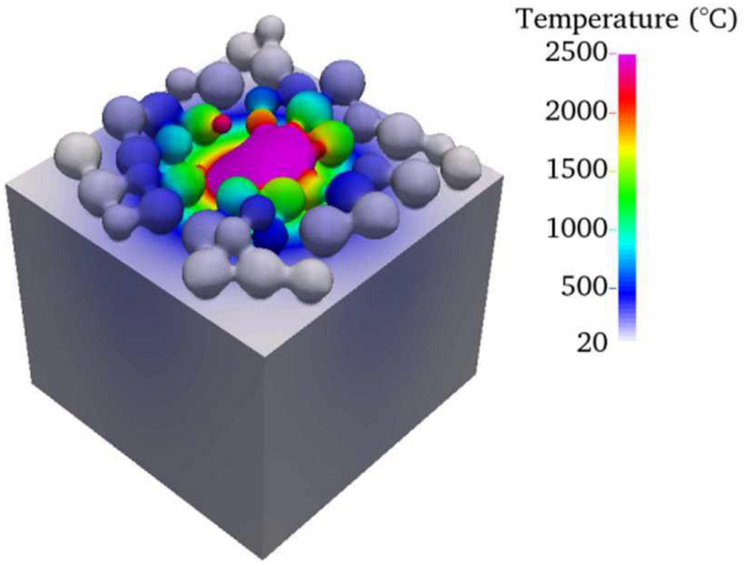

Micro-scale

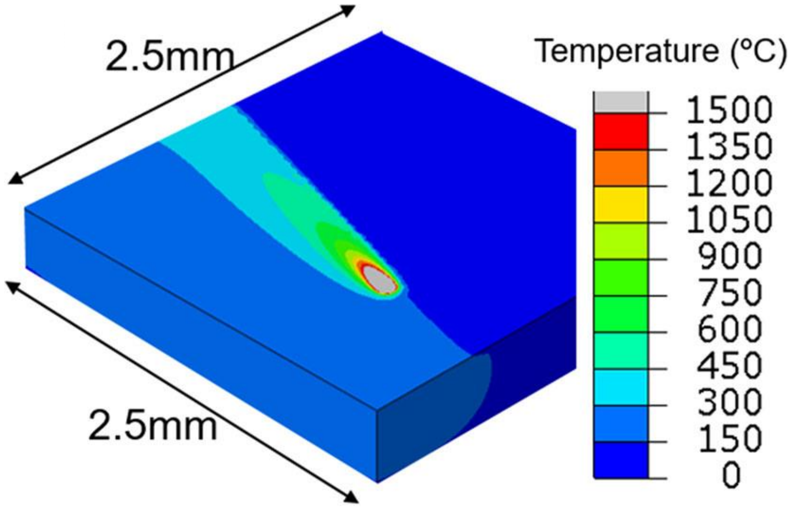

Meso-scale

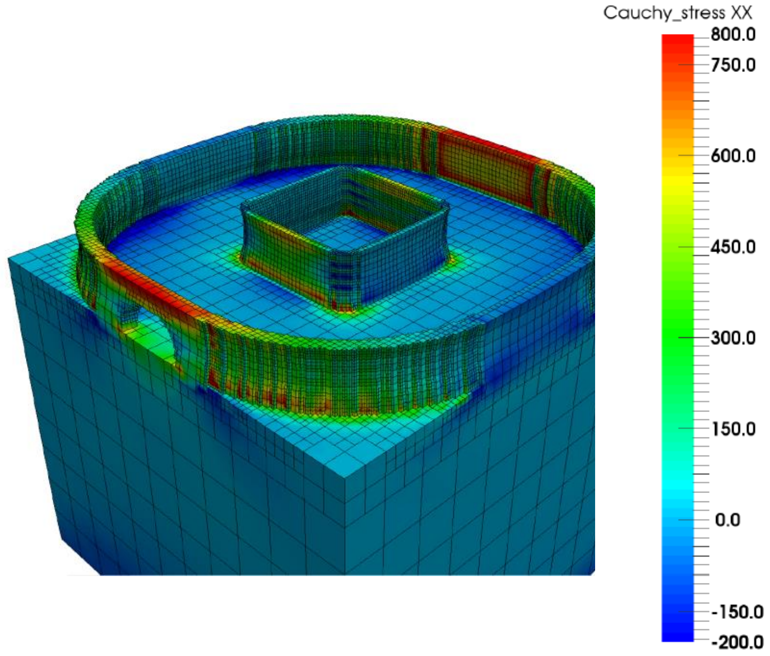

Macro-scale

Thermo-Mechanical Modeling

Heat transfer modeling

- **Heat conduction** within the solid/powder
- **Heat generated** by the laser beam
- **Heat losses** by convection/radiation

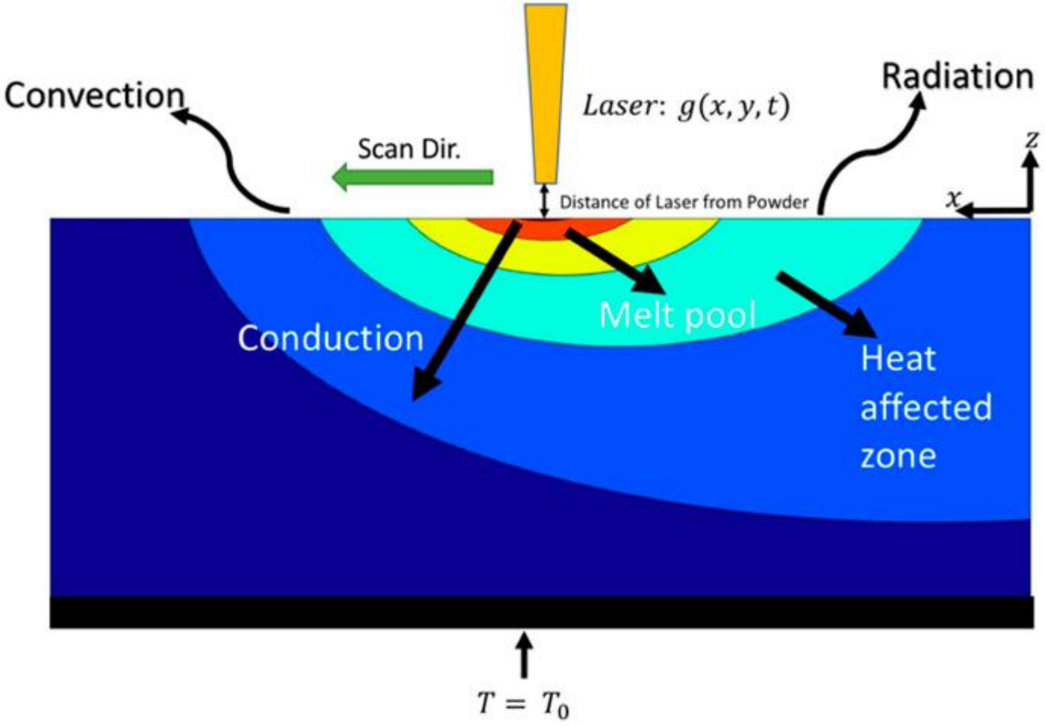

- **Transient heat conduction** within a solid material

Power generation per unit volume

Temperature

$$k\left(\frac{\partial^2 T}{\partial x^2}+\frac{\partial^2 T}{\partial y^2}+\frac{\partial^2 T}{\partial z^2}\right)+\dot{q}=\rho c_{\mathrm{p}}\frac{\partial T}{\partial t}$$

Thermal conductivity

Mass density

Specific heat

Time

Temperature dependent material properties are required

Heat transfer modeling

- Laser heat input modelled by a **volumetric Gaussian heat source**

Laser energy absorptivity — Laser power

$$\dot{q} = \frac{2^{5/2}\beta P}{\pi^{3/2} r_0^{\,3}} \exp\left\{-2\frac{x^2+y^2+z^2}{r_0^{\,2}}\right\}$$

Laser spot size

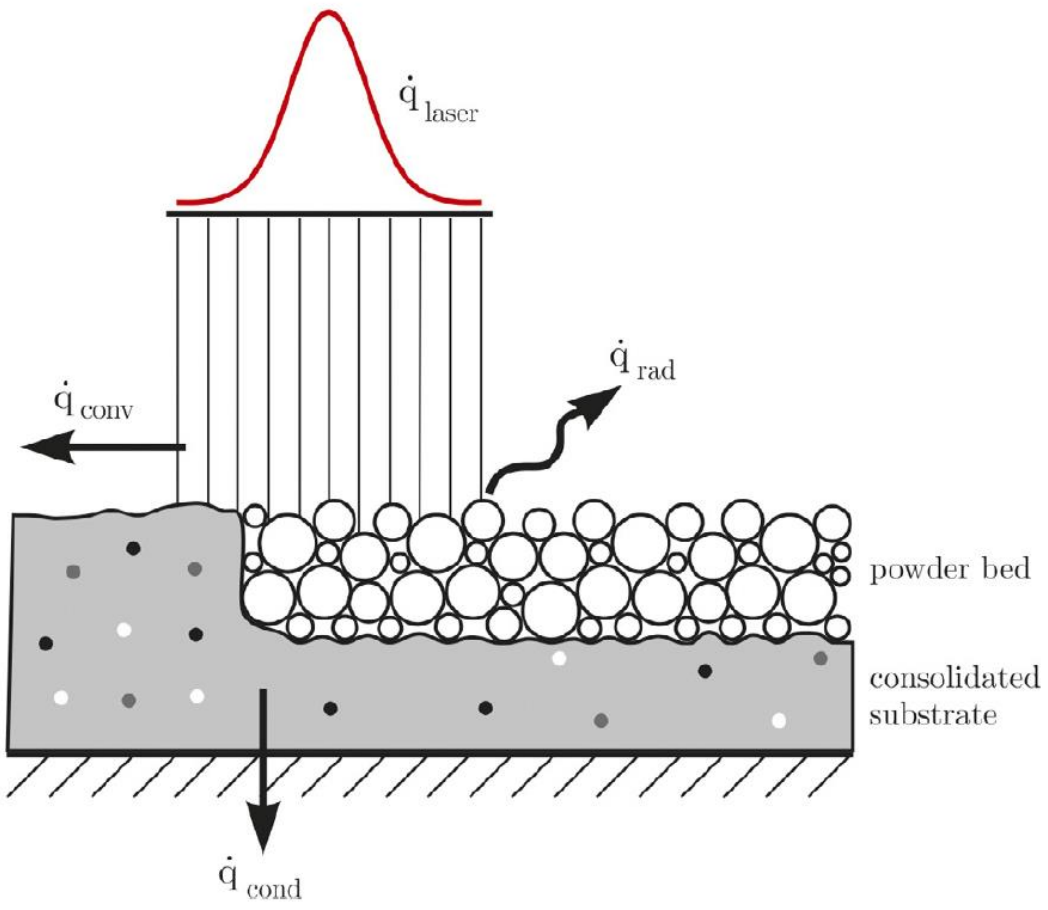

- Heat loss by **natural convection** between the exposed powder bed surface and the environment

Heat flux at the surface boundary →

$$\dot{q}_c = h_c (T - T_\infty)$$

Heat convection coefficient — Environment temperature

Mechanical modeling

- Balance of linear momentum under quasi-static analysis: $\mathrm{div}(\boldsymbol{\sigma}) + \mathbf{b} = \mathbf{0}$ (Body forces: $\mathbf{b}$; Stress tensor: $\boldsymbol{\sigma}$)
- Total strain increment: $\Delta\boldsymbol{\varepsilon}^{\mathrm{total}} = \Delta\boldsymbol{\varepsilon}^{\mathrm{e}} + \Delta\boldsymbol{\varepsilon}^{\mathrm{p}} + \Delta\boldsymbol{\varepsilon}^{\mathrm{th}}$ (Elastic strain increment: $\Delta\boldsymbol{\varepsilon}^{\mathrm{e}}$; Plastic strain increment: $\Delta\boldsymbol{\varepsilon}^{\mathrm{p}}$; Thermal strain increment: $\Delta\boldsymbol{\varepsilon}^{\mathrm{th}}$)
- **Elastic** strain: $\boldsymbol{\sigma}^{\mathrm{e}} = \mathbf{C} : \boldsymbol{\varepsilon}^{\mathrm{e}}$ (Elastic moduli: $\mathbf{C}$)
- **Plastic** strain increment:
  - Associated flow rule: $\Delta\boldsymbol{\varepsilon}^{\mathrm{p}} = \lambda \dfrac{\partial f}{\partial \boldsymbol{\sigma}}$
  - von Mises yield criteria: $f = \sigma_{\mathrm{vM}} - \sigma_{\mathrm{y}} \leq 0$
  - Swift law: $\sigma_{\mathrm{y}} = K(\varepsilon_0 + \bar{\varepsilon}^{\mathrm{p}})^n$
- **Thermal** strain: $\boldsymbol{\varepsilon}^{\mathrm{th}} = \left(\alpha_T (T - T_{\mathrm{ref}}) - \alpha_{\mathrm{ini}} (T_{\mathrm{ini}} - T_{\mathrm{ref}})\right)\mathbf{I}$ (Volumetric thermal expansion coefficients: α_T, α_{ini})

Finite Element Model

Numerical algorithms

- In-house finite element code **DD3IMP**, originally developed for sheet metal forming simulation
- Thermo-mechanical coupling using a **staggered algorithm**
- **Euler's backward time integration** for the transient heat conduction problem
- Finite deformation is described by an **updated Lagrangian scheme**
- **Fully implicit Newton–Raphson scheme** for the mechanical solution
- Thermal and mechanical solutions using the **same finite element mesh** (8-node hexahedral elements)

Finite Element Model

SLM process conditions

- **Multi-track** in a **single powder layer** deposition, scanned over solidified layers
- Material of powder and substrate: **Ti-6Al-4V**
- Finite element mesh with 10 μm of edge size
- 2 different **scanning strategies**

Process parameter	Value
Laser power [W]	83
Laser absorptivity	0.35
Laser spot radius [μm]	50
Scanning speed [mm/s]	600
Layer thickness [μm]	40
Hatching distance [μm]	120
Preheating temperature [ºC]	200

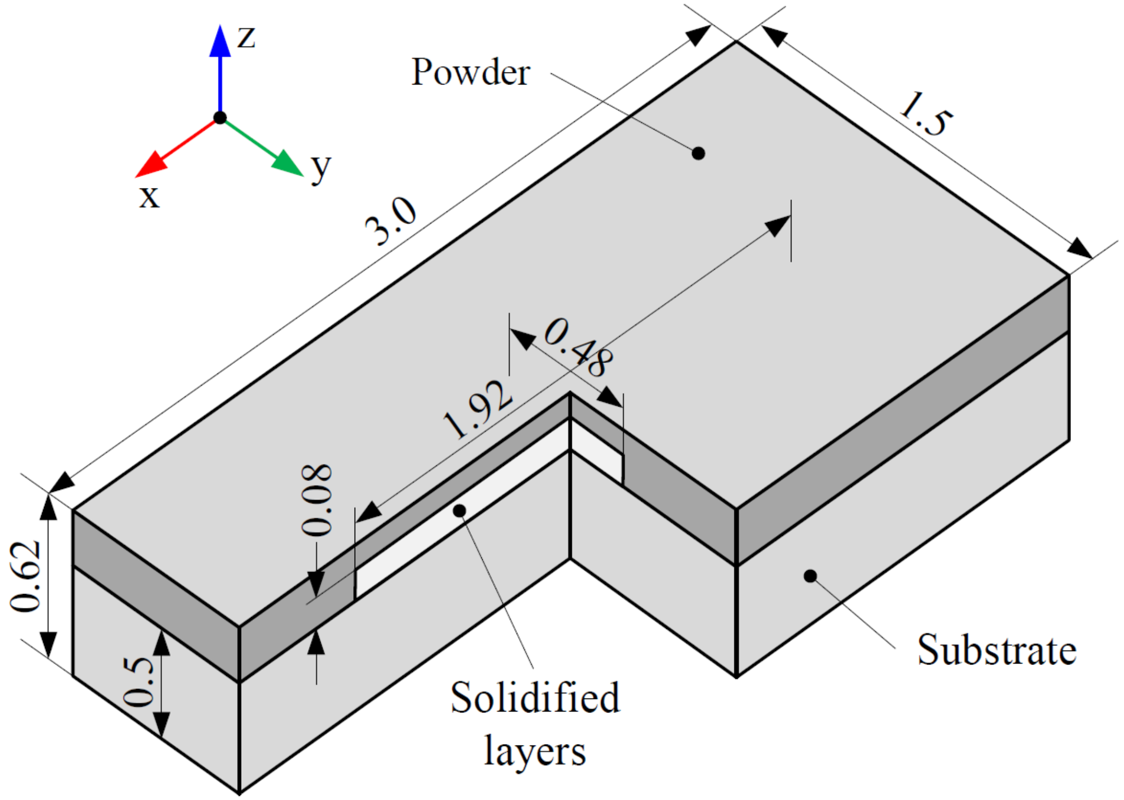

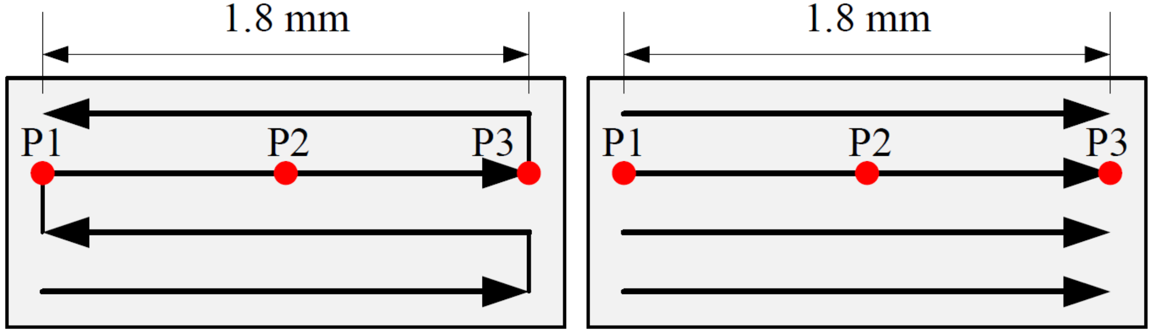

Alternating scan strategy

Unidirectional scan strategy

Thermo-physical material properties

- **Liquid with constant thermo-mechanical properties**. The thermal conductivity coefficient was artificially increased to account for the convective heat transfer within the melt pool
- Weak mechanical strength of the powder and liquid

Powder, solid and liquid Ti-6Al-4V

Property	Powder	Solid	Liquid
ρ [kg/m^3]	2600	4300	4300
c_p [J/kg·K]	-	-	820
k [W/m·K]	-	-	42
α [×10^{-6} 1/K]	1.2	12.0	0.0
E [GPa]	0.05	-	0.05
v [-]	0.34	0.34	0.34
σ_0 [MPa]	1.5	-	1.5
K [MPa]	10	-	10
n [-]	0.35	0.35	0.35

Powder Ti-6Al-4V

T [ºC]	c_p [J/kg·K]	k [W/m·K]
200	505	0.104
500	473	0.078
800	507	0.279
1000	610	0.813
1300	951	1.27
1650	1000	1.80

Solid Ti-6Al-4V

T [ºC]	c_p [J/kg·K]	k [W/m·K]	E [GPa]	σ_0 [MPa]	K [MPa]
200	566	9.3	100	630	1500
650	646	15.3	55	300	770
761	665	17.0	20	110	350
872	685	18.5	10	55	120
1094	760	24.0	3	17	60
1650	820	27.0	0.05	1.5	10

Temperature field

Unidirectional scan strategy (including cooling time)

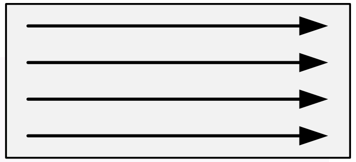

Temperature field

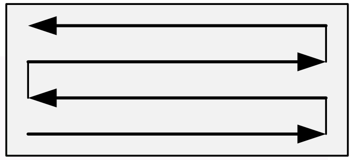

Temperature field

- Predicted **temperature field** when the laser beam is over P2 (alternating scan strategy)
- **Asymmetric temperature distribution** around the melt pool due to the low thermal conductivity of the powder
- The geometry of the melt pool is approximately semielliptical

- **Material phase status** defined by the thermal history of each finite element, using the melting temperature as bound

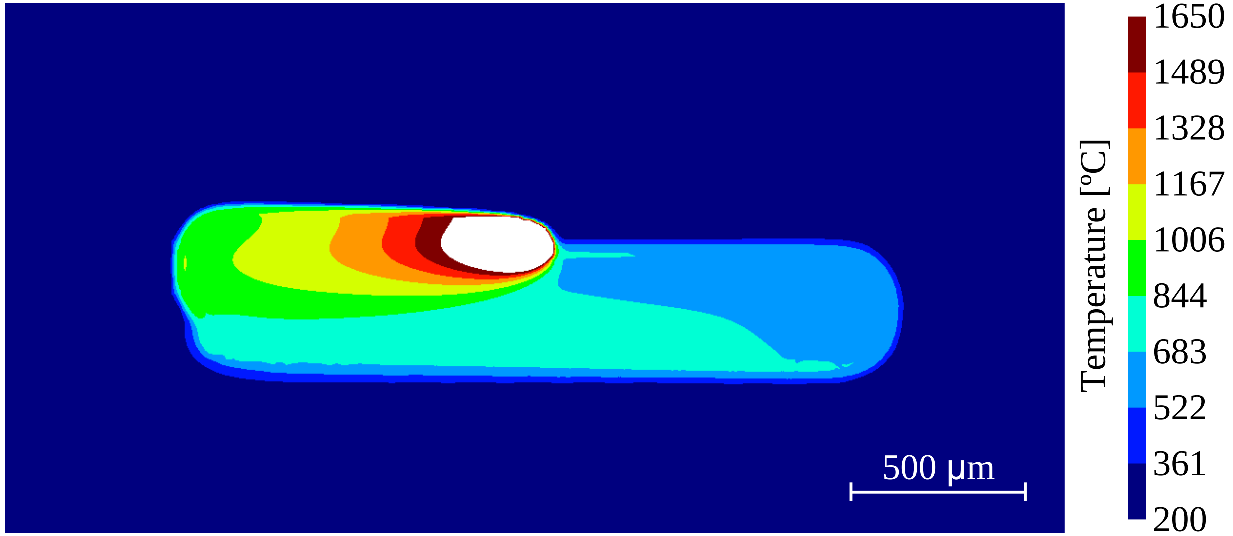

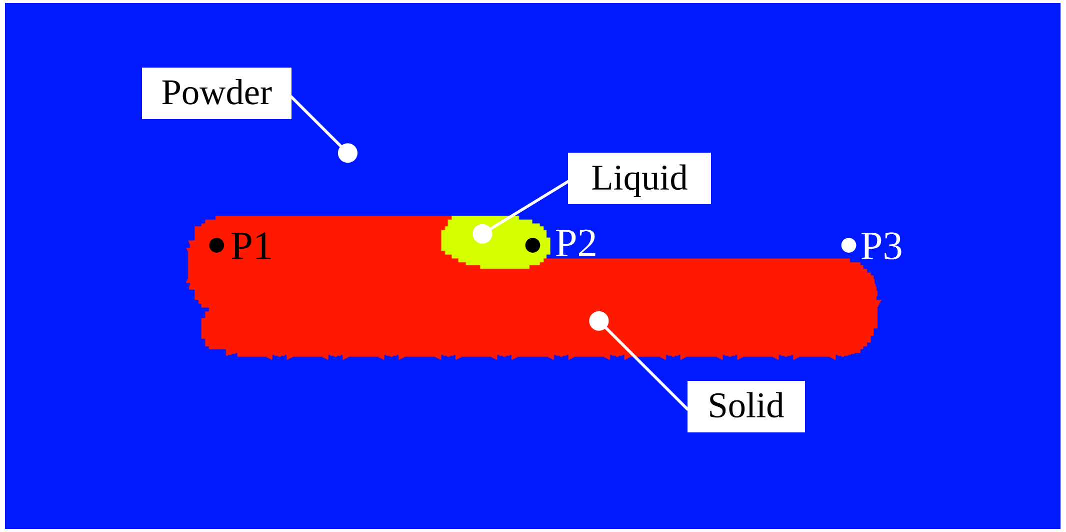

Temperature field

- The peak temperature (~3800ºC) is a singularity inside the melt pool region
- Temperature evolution in **P2** is **independent of the scanning strategy**
- The cooling down rate is identical in all points using the **alternating scan strategy**
- Larger cooling down rate at the end of the scan vector using the **unidirectional scan strategy**

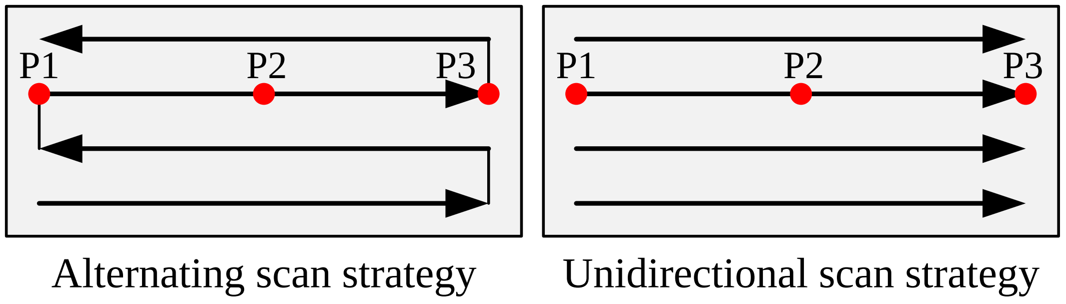

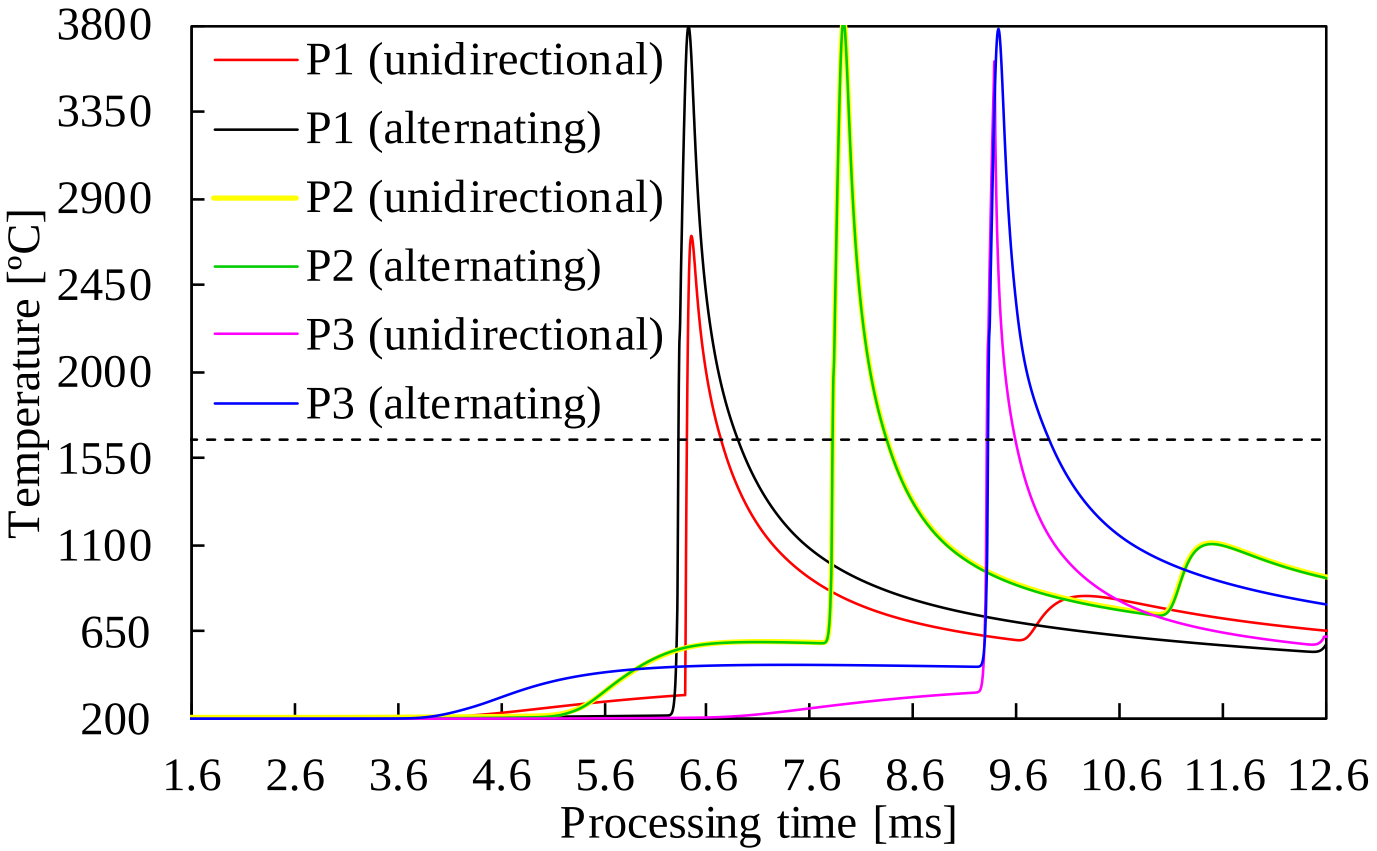

Residual stress (von Mises)

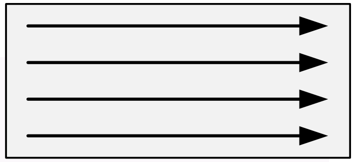

Unidirectional scan strategy (including cooling time)

Residual stress (von Mises)

Alternating scan strategy (including cooling time)

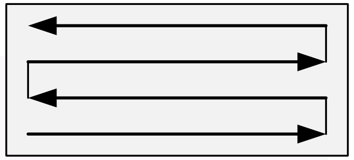

Residual stress (von Mises)

- Distribution of the **von Mises equivalent stress** in the built component after **0.5 seconds of cooling** time

Increase of the stress in the overlapping scan tracks because the accumulated plastic strain **must be withdrawn** when the material goes back to the liquid

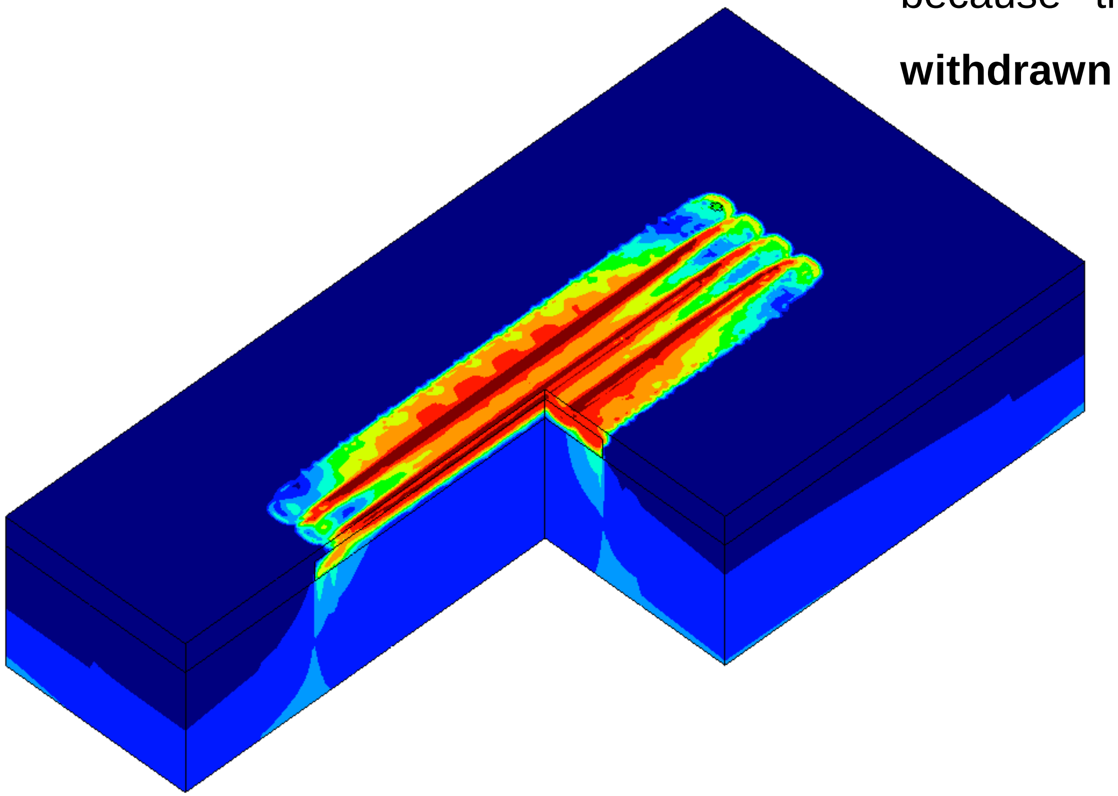

Unidirectional scan strategy

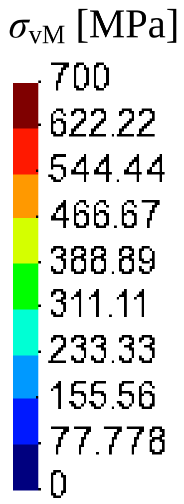

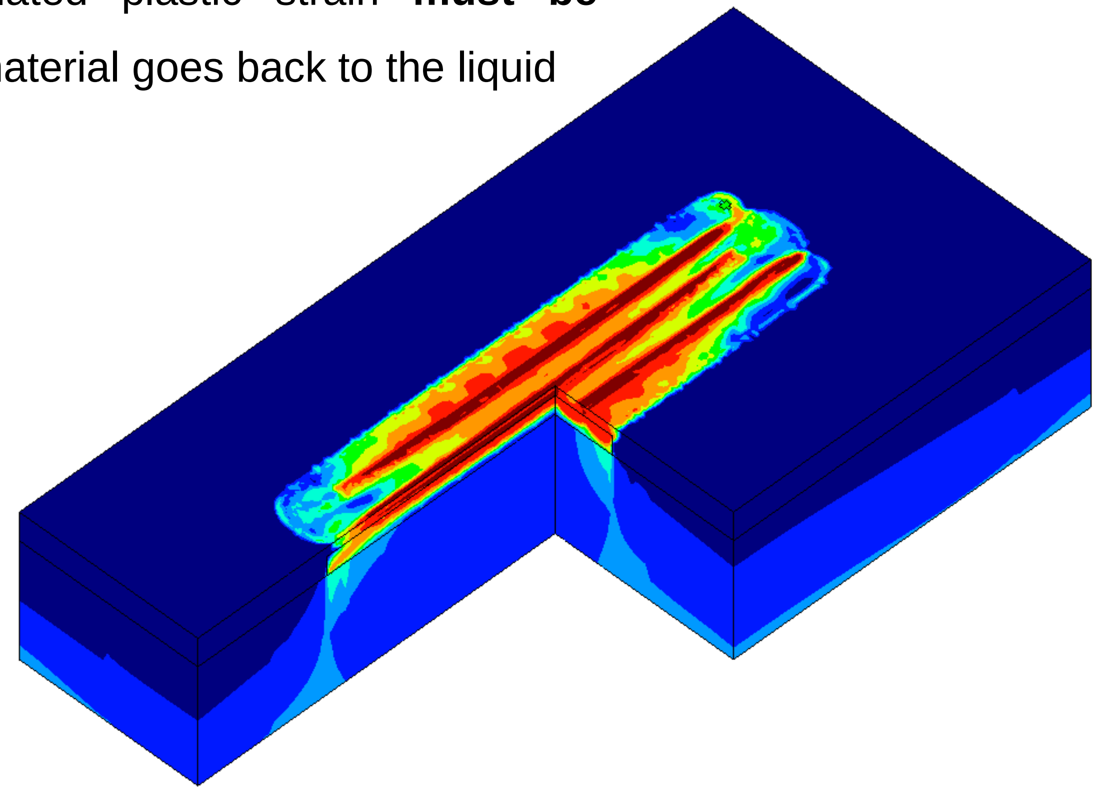

Alternating scan strategy

Results and Discussion

Residual stress (von Mises)

- **Largest stress** component arises in the direction parallel to the scanning direction
- The **longitudinal residual stress** increases considerably during the cooling
- **Positive (tension) residual stresses** in the solidified layers
- Negligible impact of the **laser scan strategy** on the residual stress field

Transverse cross-section corresponding to the half-length (unidirectional scan strategy)

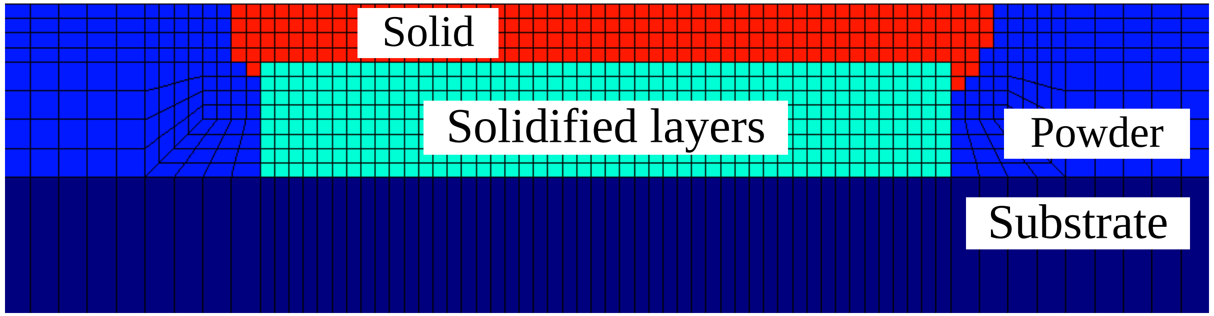

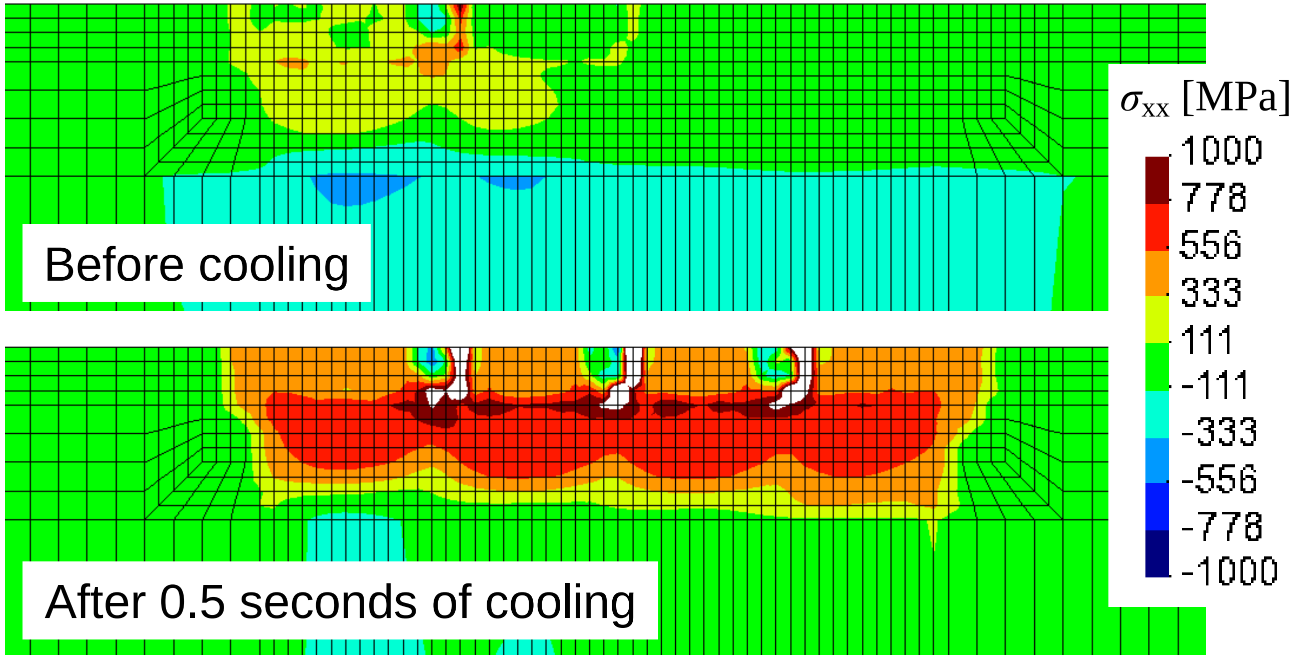

Conclusions

- **Finite element analysis** of the **selective laser melting** using a coupled **thermo-mechanical model** at meso-scale (**multi-track** in a **single powder layer** deposition)
- Transient thermal analysis and quasi-static mechanical analysis using **temperature dependent material properties**
- Influence of two different **laser scanning strategies** on the predicted residual stress
- **Shape and dimensions of the melt pool** estimated based on the predicted temperature distribution
- The residual stresses in the finished part are a result of the **non-uniform thermo-mechanical properties** (powder-liquid-solid)
- The **largest residual stress component** arises in the direction parallel to the scanning, which is **positive (tension)** in the solidified layers
- **Negligible effect of the laser scanning strategy** on the predicted stress, particularly at the mid-length of the scan vectors

Acknowledgements

This research work was sponsored by national funds from the **Portuguese Foundation for Science and Technology (FCT)** under the project with reference **PTDC/EME-EME/31657/2017** and by European Regional Development Fund (ERDF) through the Portugal 2020 program and the Centro 2020 Regional Operational Programme (CENTRO-01-0145-FEDER-031657) under the project MATIS (CENTRO-01-0145-FEDER-000014) and UID/EMS/00285/2020.

Projetos Cofinanciados pela UE:

FCT Fundação para a Ciência e a Tecnologia

CENTRO 2020

PORTUGAL 2020

UNIÃO EUROPEIA
Fundo Europeu de Desenvolvimento Regional

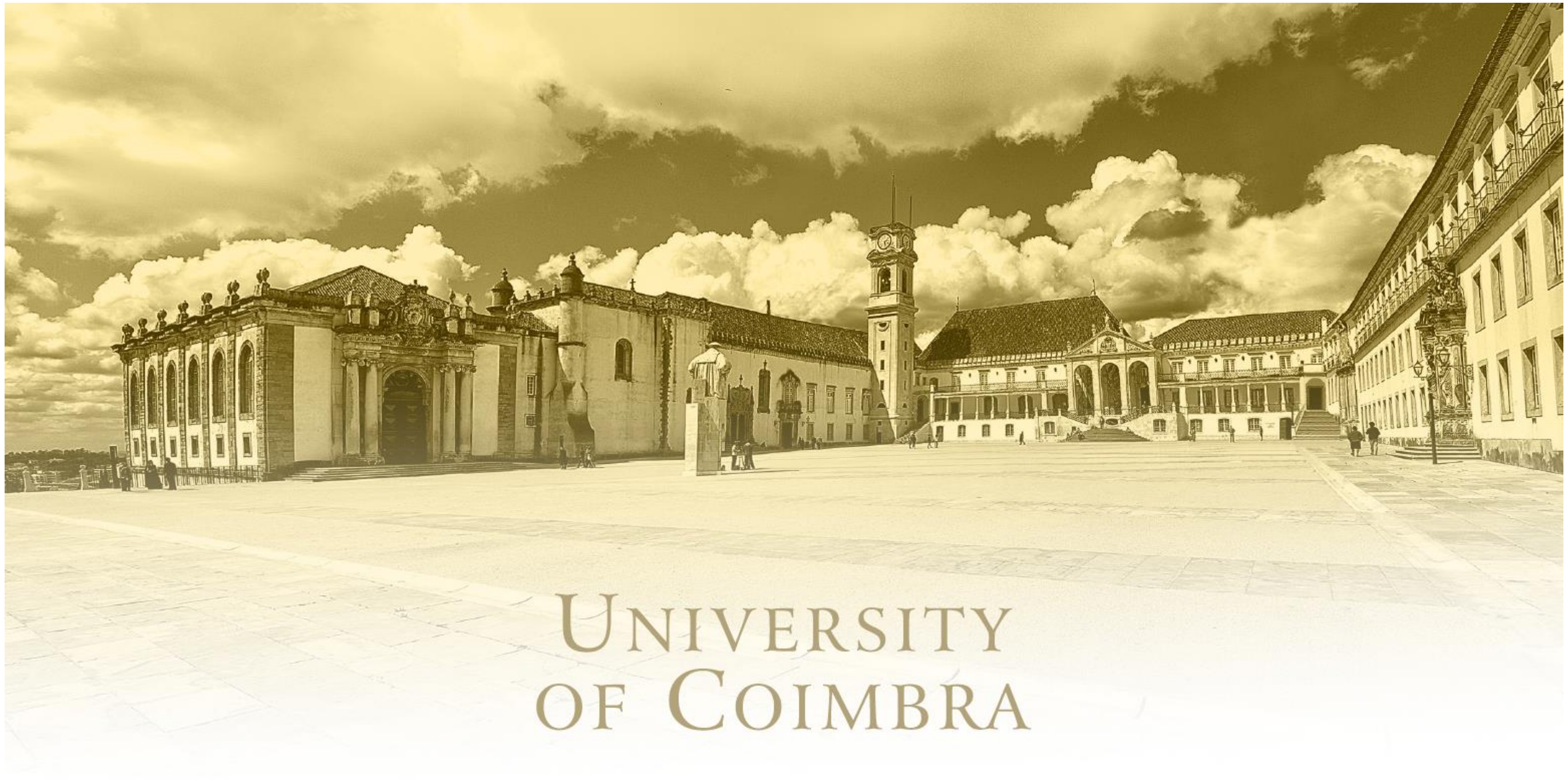

Thank you for watching!